ORIGINAL RESEARCH

3D Numerical Modeling of Seismic-Induced Settlement of Pile Groups in Liquefiable Sands

Shima Aghakasiri [1], *, Sanaz Aghakasiri [2], Mahmoud Ghazavi [3], Farzad Farrokhzad [4], Saeed Farrokhizadeh[5]

[1] Department of Civil Engineering, S.T.C, Islamic Azad University, Tehran (Iran) ; sh.aghakasiri@iau.ir

[2] Department of Civil Engineering, Babol Noshirvani University of Technology (NIT), Babol, Mazandaran, (Iran) ; sanazaghakasiry@gmail.com

[3] Department of Civil Engineering, K.N. Toosi University of Technology, Tehran (Iran) ; ghazavi_ma@kntu.ac.ir

[4] Department of Civil Engineering, Mazandaran Institute of Technology, Mazandaran (Iran) ; farzadfarokhzad@mit.ac.ir

[5] Department of Civil Engineering, S.T.C, Islamic Azad University, Tehran (Iran) ; s_farrokhizadeh@azad.ac.ir

*Correspondence: sh.aghakasiri@iau.ir

Received: ; **Accepted:** ; **Published:**

Citation: Agha kasiri, Sh. Agha kasiri, S. Ghazavi, M. Farrokhzad, F. Farrokhizadeh, S. (2025). 3D Numerical Modeling of Seismic-Induced Settlement of Pile Groups in Liquefiable Sands. INTERNATIONAL JOURNAL OF ADVANCED STRUCTURAL. https://doi.org/

Abstract: During historical seismic events, soil liquefaction beneath structures founded on shallow foundations has caused substantial economic losses. As reported in various case histories, structures located on liquefiable soils experience excessive settlement, tilting, and significant lateral deformation due to the low bearing capacity of such soils. Seismic-induced ground deformation in liquefiable soils poses significant challenges to the stability and serviceability of pile-supported structures. This study presents a comprehensive three-dimensional numerical investigation into the settlement behavior of pile groups embedded in liquefiable sands under seismic loading. Using the finite difference-based software FLAC3D, the coupled effects of soil liquefaction, excess pore water pressure generation, and dynamic soil-structure interaction were considered. Parametric analyses were conducted to assess the influence of pile spacing, group configuration, and input motion characteristics on the magnitude of post-earthquake settlement. The results highlight the critical role of 3D interaction effects in amplifying or mitigating the settlement response. This study provides valuable insights into the design and performance assessment of deep foundations in liquefaction-prone areas.

Keywords: 3D numerical modeling, Liquefaction, settlement, Pile groups, Soil-structure interaction, Finite difference method, pore pressure, Earthquake engineering

Highlights:

- Numerical pile–soil interaction modeling was performed using FLAC 3D with the Finn liquefaction model under near-field and far-field seismic loading.
- Far-field earthquakes generated more severe liquefaction and greater pile group settlement compared to near-field events.
- Vertical ground motion components significantly increased liquefaction-induced settlement in saturated sandy deposits.
- Sensitivity analysis identified optimal mesh size and boundary conditions to balance computational efficiency and model accuracy.
- Practical implications suggest that pile cap design and shaft friction behavior in liquefiable soils require further research, especially for different pile cross-sections.

1. Introduction

Liquefaction is a critical phenomenon in saturated soils that occurs under intense cyclic dynamic loading, such as major earthquakes. Under undrained conditions, the buildup of excess pore-water pressure can reduce the effective stress of the soil to a level at which the soil behaves like a fluid and can no longer sustain shear forces. This condition arises when the ratio of excess pore-water pressure to the initial effective confining stress (PL/σ′) approaches unity, or when the cyclic shear strain amplitude reaches a critical threshold [1]. In such cases, loose, liquefaction-susceptible soils may exhibit significant changes in seismic response, including shifts in natural frequencies, amplification of frequencies below 1 Hz, and attenuation of higher frequencies [2].

Liquefaction is recognized as a geohazard with devastating consequences; its occurrence often leads to bridge foundation settlements, structural collapse, and slope instability, posing serious threats to life and property [3, 4]. Numerous seismic records indicate that liquefaction is one of the most destructive consequences of earthquakes, often resulting in irreversible damage [5]. Notable examples include the destructive liquefaction effects observed in the 1964 Niigata earthquake, the 2010 Maule (Chile) earthquake, the 2010 & 2011 Christchurch (New Zealand) earthquakes, the 2011 Tōhoku (Japan) earthquake, the 2012 Emilia Romagna (Italy) earthquake, and the 2018 Sulawesi (Indonesia) earthquake [6-13]. Figure 1 illustrates the damage to buildings and infrastructure caused by soil liquefaction in various parts of the world.

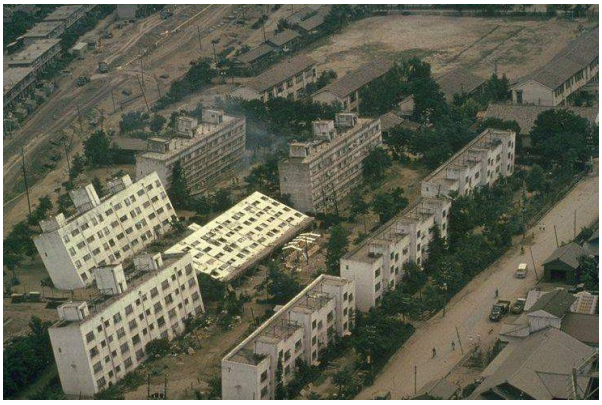

Figure 1. group of apartment building in kawagishi-cho in nigata 1964[14]

The process of liquefaction involves the transformation of soil from a solid state to fluid-like behavior under dynamic loading due to the reduction of effective stress caused by excess pore-water pressure [15, 16]. During strong earthquakes, particularly when there is insufficient time for the dissipation of pore-water pressure, the hidden compression within the soil structure decreases, transferring stress to the water in the pores. This accelerates the loss of shear strength. If this reduction in shear strength surpasses the applied shear stress, the soil undergoes liquefaction, leading to significant deformations [17].

This phenomenon poses heightened technical challenges in developed areas constructed on liquefaction-prone soils, such as buildings, bridges, and buried infrastructure [18]. The expansion of urban areas and the growing demand for infrastructure development often result in construction on reclaimed land or

riverbeds filled with locally sourced sand and gravel materials that can be susceptible to liquefaction.

Liquefaction may be triggered by various factors, including earthquakes, rising groundwater levels, excessive loading, machinery vibrations, and cyclic loading [19]. In this phenomenon, the shear strength and stiffness of the soil are significantly reduced, often causing damage to critical infrastructure [20, 21]. For example, Esfeh et al. (2019) demonstrated through numerical modeling that piles supporting offshore structures may experience permanent lateral displacement and tilting due to the combined effects of dynamic loading and liquefaction [22]. Furthermore, several studies have investigated the effects of pile geometry, pile-group configurations, shallow foundation settlements, and the seismic response of substructures in liquefiable soils, highlighting the importance of detailed numerical analyses in this field [23-35]. In 2024, Chi et al. investigated the numerical and experimental modeling of dynamic responses of permeable piles in liquefied sandy soil using Falc 3D software[36]. Reyes et al. investigated the application of the SANISAND-MSf structural model to simulate cyclic liquefaction in FLAC2D and FLAC3D software[37]. Although these methods remain valuable for preliminary evaluation, they often neglect the nonlinear and three-dimensional nature of soil–structure interaction (SSI) under seismic loading. Simplified analytical methods, such as p–y or t–z curve formulations, are also limited in capturing the complex load transfer mechanisms and stiffness degradation in liquefied layers.

Although numerous studies have examined liquefaction and pile response, most previous works have focused on 2D analyses or single-pile behavior. Few studies have investigated 3D dynamic interaction under near- and far-field earthquake conditions. Therefore, this study aims to develop a comprehensive 3D numerical model in FLAC3D to assess the settlement behavior of pile groups in liquefiable sands, considering the coupled effects of pore pressure generation and dynamic loading.

Understanding the seismic performance of pile groups in liquefiable soils is essential for the design of deep foundations in earthquake-prone regions such as Japan, Iran, and New Zealand. This research contributes to improving the reliability of design guidelines by quantifying the influence of earthquake frequency content, pile spacing, and soil properties.

In developing countries like Iran and Japan, where critical infrastructure is often built on reclaimed or alluvial deposits, understanding liquefaction-induced settlement in pile-supported systems is of great practical importance. The current study aims to perform a comprehensive three-dimensional numerical analysis using FLAC3D to evaluate the seismic settlement behavior of pile groups in liquefiable sands. The model incorporates coupled dynamic and liquefaction analyses based on the Finn model and investigates the effects of pile spacing, earthquake motion characteristics, and soil permeability. The findings of this research are expected to provide valuable insights into the design and seismic performance assessment of deep foundations in liquefaction-prone regions.

2. Liquefaction and Pile Behavior Based on SPT Data (Traditional Methods)

Traditional evaluation of soil liquefaction and its effects on pile foundations has primarily relied on empirical and deterministic methods derived from in-situ tests such as the Standard Penetration Test (SPT). The pioneering approaches developed by Seed and Idriss (1971) and later refined by Youd et al. (2001)

established simplified procedures for estimating the cyclic resistance ratio (CRR) and comparing it with the cyclic stress ratio (CSR) to assess liquefaction potential[1, 38].

These classical frameworks assume that soil response under cyclic loading is largely predictable through correlations between corrected SPT blow counts $N_{1(60)}$ and empirical safety factors. However, the deterministic nature of these methods limits their ability to capture the nonlinear, site-specific, and stress-dependent behavior of saturated granular soils.

Moreover, in the case of pile foundations in liquefied ground, traditional methods such as p-y, t-z, and q-z curves or simplified beam-on-Winkler models cannot fully represent the complex soil–pile interaction under dynamic and post-liquefaction conditions (e.g., lateral spreading, loss of stiffness)[39, 40].

Therefore, while empirical and analytical procedures remain valuable for practical design and preliminary assessment, their accuracy strongly depends on empirical correlations and regional calibration, often leading to uncertainty in predicting pile performance in liquefied layers.

3. Evaluation of Liquefaction-Induced Settlement and Differential Deformation

In addition to triggering analyses, liquefaction-induced settlement and differential deformation represent critical concerns in geotechnical earthquake engineering due to their potential to compromise the integrity of foundations and structures.

Several empirical and semi-empirical approaches have been proposed to estimate post-liquefaction settlements, including those by Tokimatsu and Seed (1987), Ishihara and Yoshimine (1992)[41, 42]. These methods typically involve evaluating the cyclic shear stress ratio (CSR), estimating the corresponding volumetric strain ε_v through empirical relationships or charts, and integrating these strains over the liquefied layers to compute total settlement:

$$S=\sum(\varepsilon_{v_i}, h_i) \quad (1)$$

where S denotes the total settlement, ε_{v_i} is the volumetric strain for the i-th layer, and h_i represents the thickness of that layer. Figure 2 illustrates the relationship between the cyclic stress ratio (CSR), corrected SPT blow count $N_{1(60)}$, and the resulting volumetric strain.

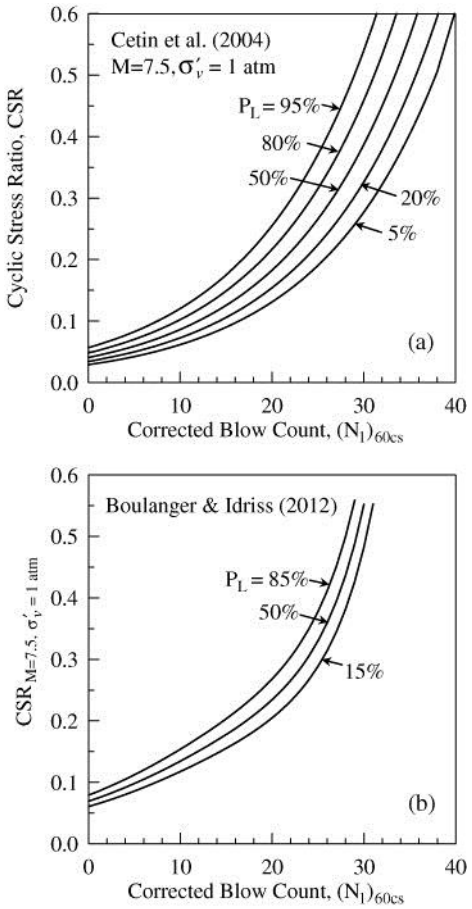

Figure 2. SPT-based probability contour curves: (a) Cetin et al. (2004), and (b) Boulanger and Idriss (2012) [43, 44]

The calculated settlements obtained from various empirical methods are summarized in Table 1. As expected, uniform liquefaction-induced settlements rarely cause significant

structural damage; however, differential settlements pose a more severe threat due to non-uniform ground deformation.

Table 1. Settlements induced by liquefaction estimated using different methods

different methods	Settlement (m)
Tokimatsu and Seed (1987)	21
Ishihara and Yoshimine (1992)	40
Wu and Seed (2004)	25
Average settlement	28.66

For practical engineering design, the magnitude of differential settlement is generally approximated as 50% of the total estimated settlement, which provides a reasonable representation of post-liquefaction deformation effects in routine analysis and design.

4. Numerical Modeling of Piles in FLAC 3D Using the Pile Element

FLAC is based on the finite difference method (FDM) using an explicit Lagrangian scheme, rather than the finite element method (FEM). While FEM discretizes the domain into elements with shape functions, FDM approximates the governing differential equations through finite difference operators on a numerical grid. This makes FLAC particularly efficient for modeling large deformations and nonlinear geotechnical problems.

In FLAC 3D, the pile structural element is used to simulate the frictional interaction between nodal points and the pile structure in both directions perpendicular and parallel to the pile axis. In addition to representing shaft friction, this element allows the modeling of end-bearing resistance. The properties of the pile structural element are categorized into two groups:

$$\frac{F_s^{\max}}{L} = cs\_scoh + \sigma_m . p . \tan(\text{cs\_}s\ \text{fric}) \quad (2)$$

$$u_s = \frac{\frac{F_s^{\max}}{L}}{cs\_sk} \quad (3)$$

(2) geometric and physical properties of the pile, and (3) parameters defining the interaction between the grout around the pile and the surrounding soil.

The scoh cs parameter represents the grout adhesion strength per unit length. The maximum unit shear resistance is computed using Equation (2), while the pile's shear displacement prior to reaching maximum shear capacity is calculated using Equation (3).

5. Evaluation of Pile Group Bearing Capacity Under Vertical Loading

When multiple piles are arranged as a pile group, the stress zones in the surrounding soil arising from both shaft friction and end-bearing may overlap. The magnitude of this stress depends on the applied live load and the pile spacing. If the induced stresses are high enough, the soil may undergo shear failure or experience excessive settlement. The degree of stress overlap decreases significantly with increased pile spacing (S).

According to the BOCA (1993) code[45], in loose sand or loose sandy gravel, interior pile spacing should be increased by 10–40%. For vertical loads, the optimum spacing is approximately 2.5–3.5 times the pile diameter (D), while in certain special projects, spacings of 8–10D are used, as referenced by Bowles. Fotch and oneil (1985) recommended the use of the Cumulative Distribution Function (CDF) approach for pile installation [46]. In this study, the Converse–Labarre equation was applied to compute the pile group efficiency (Equation 4).

$$E_g = 1 - \theta\ \frac{(n-1)m + (m+1)n}{90mn} = 0.72 \quad (4)$$

In Equation (4), the group efficiency is determined using the number of rows (n), the

number of columns (m), the pile diameter (D), and the parameter ϕ calculated in radians from Equation (5). In Equation (5), S denotes the pile spacing. This formulation applies to rectangular pile groups with distinct m × n arrangements, as illustrated in Figure 2 for a five-pile group configuration.

$$\theta = tg^{-1}\frac{D}{S} \quad (5)$$

Using the Converse–Labarre equation along with CDF recommendations, the group efficiency is determined and then used in Equation (6) to calculate the total group bearing capacity.

$$Q_g = N_p Q_p E_g = 2160\ ton \quad (6)$$

The stress bulb beneath the pile tip diminishes with distance, but becomes more pronounced under higher loading due to increased relative displacement between the pile tip and soil, activating the tip resistance. The figure 3 illustrates that the pile behaves as a rigid body with uniform displacement, while the soil beneath exhibits varying stress contours.

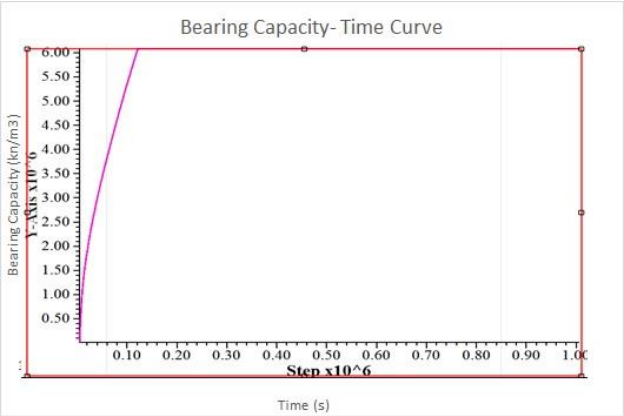

Figure 3. Pile bearing capacity considering the shaft friction effect based on the Mohr-Coulomb model

6. Pile and Soil Modeling in FLAC 3D

The selected constitutive model for the soil in static conditions was the Mohr–Coulomb model, while the Finn model was adopted for dynamic and liquefaction simulations. The groundwater table was assumed at a depth of 2 m. Under dynamic loading conditions, the primary focus was on the load–settlement response of the pile. The parameters required for the numerical analysis are presented in Table 2. Pile and soil modeling shown in figure 4.

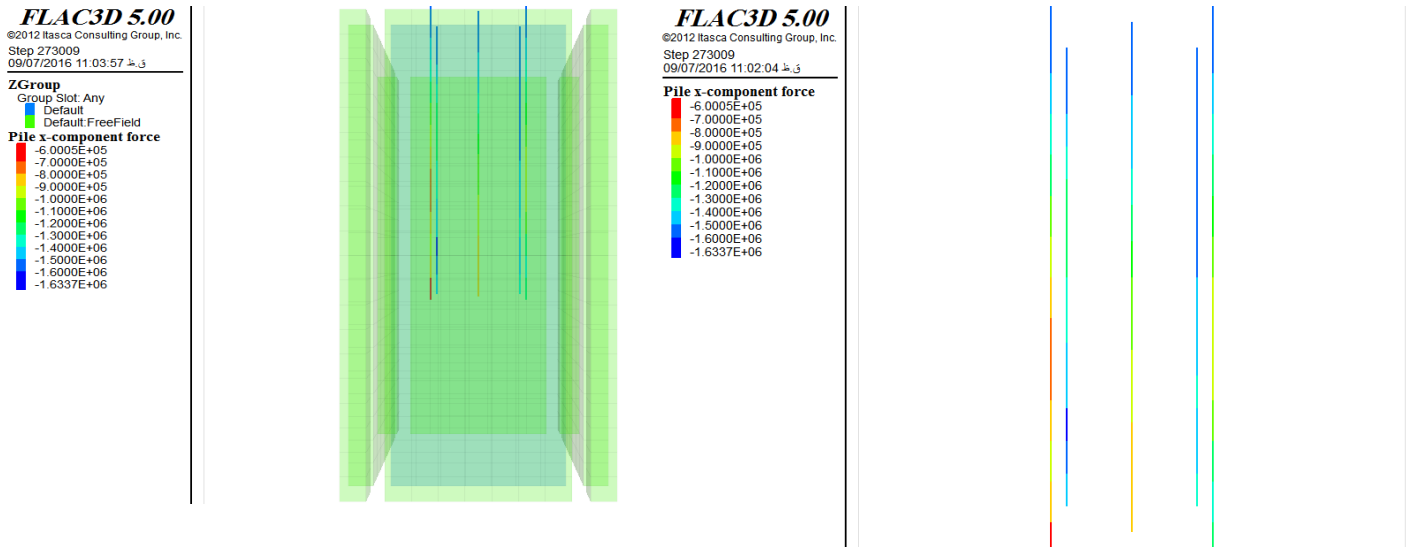

Figure 4. Pile and Soil Modeling in FLAC 3D

Table 2. Geotechnical parameters used for numerical analysis

Layer tickness (m)	$\gamma_d \frac{kg}{m^3}$	C	Φ	n	$N_{1(60)}$	Bulk modulus(mpa)	Shear modulus(mpa)
2	1750	0	28.7	0.46	9	28.85	57.7
2	1538	0	30.00	0.42	7.2	21.6	27
2	1910	0	27.2	0.43	22	29.5	59.01
2	1870	0	28.3	0.42	28	29.97	59.95
2	2020	0	26.4	0.48	52	30.5	61.00
2	1840	0.07	25.3	0.49	14	30.49	60.99
2	1930	0.02	26.2	0.44	39	31.74	63.49
2	2021	0	27.3	0.41	90	32.29	64.59
4	2010	0.02	28.2	0.39	85	31.00	62.00

7. Dynamic Analysis of the Model

Dynamic analyses were performed using earthquake acceleration records obtained from the PEER database (Tables 3 & 4), representing both near-field and far-field motions.

The selected time histories were filtered using SEISMO SIGNAL software, and baseline correction was applied before introducing the stress history at the base boundary of the model. Six near- field and far- field accelerograms, along with their station information and moment magnitudes, were selected for the analysis.

Table 3. Earthquake parameters (Near fault acceleration)

Earthquake	Site station	Year	Distance from the fault (km)	M_W
Superstition Hills	PTS	1987	1.00	6.5
Northridge	LAD	1994	5.9	6.7
Loma Prieta	CSMIP Carralitos	1989	2.8	6.9

Table 4. Earthquake parameters (Far fault acceleration)

Earthquake	Site station	Year	Distance from the fault (km)	M_W
Imperial Valley	Holtville-post office (USGS)	1979	25.7	6.4
Duzce	SKR	1999	65	7.2
Kobe	Shin-osaka (CUE)	1995	19.2	6.9

A total of six earthquake records were employed three near-field and three far-field and their effects were compared. Figures 5 through 10 present the velocity–time histories of the selected ground motions.

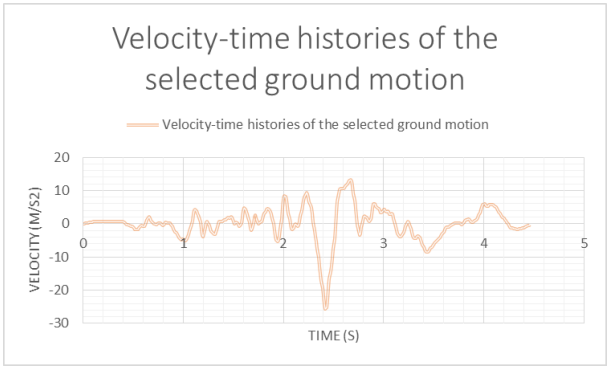

Figure 5. Superstition Hills earthquake

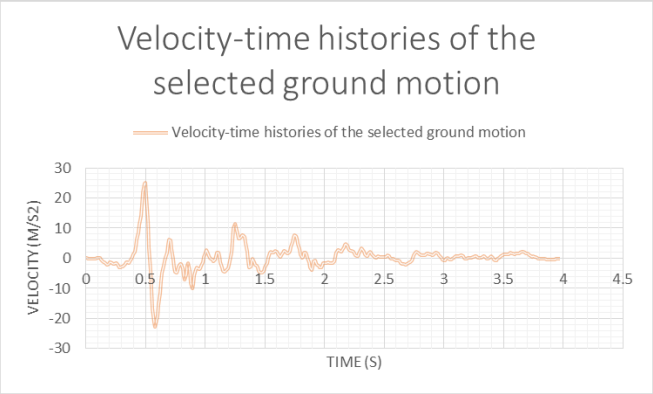

Figure 6. Northridge earthquake

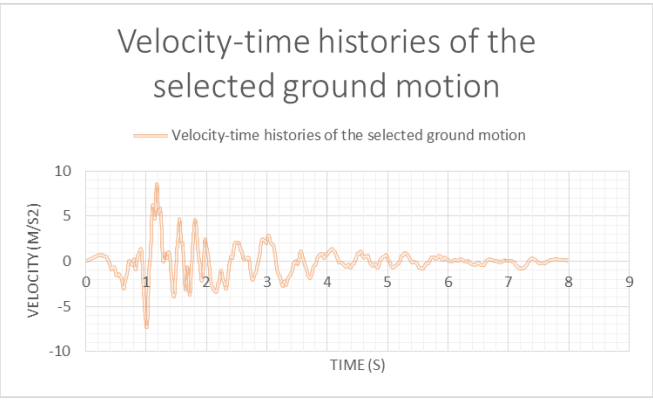

Figure 7. Loma Prieta earthquake

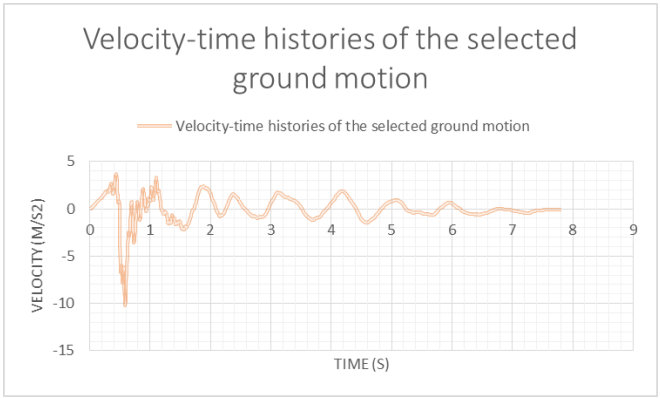

Figure 8. Imperial Valley earthquake

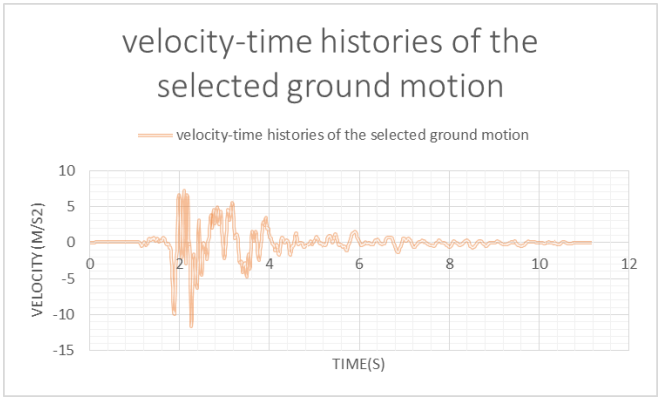

Figure 9. Duzce earthquake

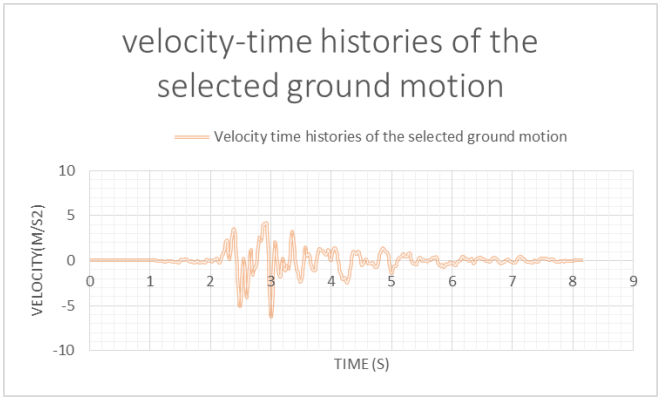

Figure 10. Kobe earthquake

Upon execution, the calculated bearing capacity of the pile–soil system was found to be 600 tons. The results indicate that the pile element behaves as a rigid body, exhibiting uniform displacement, while the surrounding soil shows varying stress contours. As the distance from the pile tip increases, the stress bulb beneath the tip decreases. At higher load levels, the stress bulb at the pile tip becomes more distinct, due to the increased relative displacement between the pile tip and the surrounding soil, thereby mobilizing end-bearing resistance.

Figures 11 display the settlement of the soil in the pile group under near-field and far-field earthquakes. The results demonstrate that far-field earthquakes induce more severe liquefaction in sandy soils compared to near-field events, leading to greater pile group settlement under similar conditions.

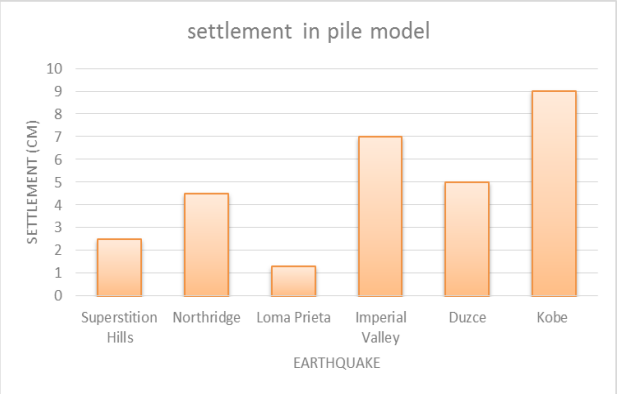

Figure 11. settlement in pile group modeling

8. Sensitivity Analysis of the Model

The primary objective of the sensitivity analysis is to develop a reduced-size model that minimizes computational time while maintaining accuracy. Although the real soil domain is theoretically infinite, numerical modeling imposes limitations on model dimensions. Some software packages allow for boundary conditions that approximate infinite domains; however, FLAC lacks this capability. Therefore, the model boundaries must be defined such that they are sufficiently large to avoid stress influence while remaining computationally efficient.

When the lateral boundaries are too close to the pile, the surrounding stress field is affected. Conversely, increasing the distance excessively results in longer run times. An optimal domain size must therefore be determined to minimize negative effects while maintaining computational efficiency. The purpose of maintaining adequate spacing between the pile and lateral boundaries is to ensure that stress irregularities do not occur in the horizontal direction.

For defining boundary conditions in the vertical direction, a virtual boundary is applied, constraining nodes along the Z-direction to prevent movement thereby enforcing a plane strain condition. The required distance between the pile tip and the vertical boundary depends on whether the pile is classified as long or short. Based on the relationships and findings from this study, the piles under consideration are classified as long piles.

The validation model was adapted from the study by Halder and Babu [47], which examined the seismic behavior of piles in liquefiable deposits under varying relative densities. The soil profile considered had a depth of 20 m and a lateral width of 40 m, consisting of a homogeneous saturated sand layer. The mesh was discretized into 20 rows and 20 columns, forming 400 quadrilateral zones with a maximum element size of 1.33 m. The pile length was 21 m, with 20 m embedded and 1 m above ground. The pile was seated on bedrock and was thus restrained only in the vertical direction. Superstructure effects were modeled by applying an equivalent vertical load, along with a horizontal load equal to 10% of the vertical load to account for superstructure inertia.

Material properties for the soil and pile were taken from Liyanapathirana and Poulos [48]The selected earthquake records (Table 5) were scaled to a peak ground acceleration (PGA) of 0.2g.

Table 5. Earthquake parameters **(Far fault acceleration)**

Earthquake	Year	Dominant frequency(HZ)	PGA	M_W
Kobe	1995	9.9	0.2g	6.9

Based on the maximum element size of 1.33 m, the maximum allowable frequency passing through the mesh was calculated using Equation (7) [48] to be 9.9 Hz. Consequently, the earthquake records were filtered to 9 Hz, removing higher frequency components while retaining the earthquake energy content. Baseline correction was applied linearly, and the Finn model was implemented for liquefaction simulation, with hysteretic damping adjusted from FLAC's default settings to accommodate large shear strains.

$$f = \frac{v_s}{\Delta l * 10} \quad (7)$$

To mitigate undesirable wave reflections within the model, free-field boundaries were implemented. Upon attaining mechanical equilibrium and transitioning the soil behavior from the Mohr–Coulomb constitutive model to the Finn model, incorporating appropriate hysteretic damping, the dynamic analysis was performed using a time-history of horizontal acceleration applied at the bed boundaries.

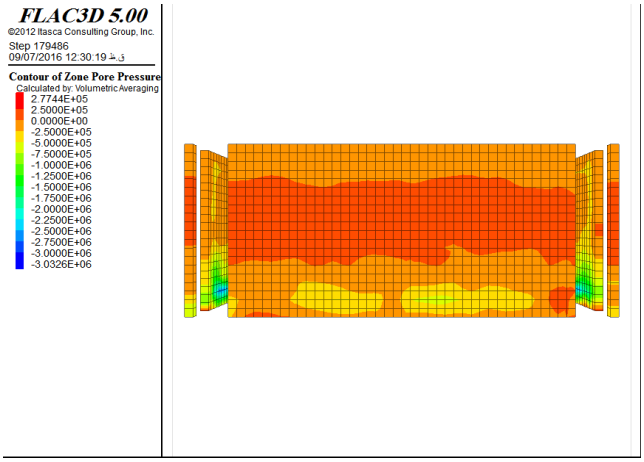

Figure 12. Liquefaction in the 20×40 model

As anticipated, liquefaction initiates below a depth of 4 meters, in agreement with the findings reported in the referenced study, as illustrated in Figure 12.

9. Explain about fault and near acceleration

Piles are essential for resisting settlement in buildings, bridges, and other infrastructure, especially in loose sandy deposits subject to seismic loading. Earthquakes can generate excess pore-water pressure in saturated or loose saturated sand, significantly reducing shaft friction and end-bearing capacity, leading to pile settlement.

This study employed FLAC 3D numerical modeling to assess the effects of input motion frequency content and vertical motion amplitude on the settlement of pile groups in saturated sands. The influence of soil permeability on the seismic pile–soil response was also investigated. Results showed that far-field earthquakes induce more severe liquefaction and higher settlement compared to near-field motions. Moreover, vertical ground motion significantly amplifies liquefaction-induced settlement.

The settlement values presented here are derived from field observations and previously published studies:

The evaluation of liquefaction-induced settlements under different seismic scenarios highlights a clear distinction between near-field and far-field earthquakes. In near-field events, such as Superstition Hills (1987), Northridge (1994), and Loma Prieta (1989), the presence of strong velocity pulses leads to a rapid build-up of excess pore water pressure and the onset of liquefaction within a relatively short duration. Consequently, the observed settlements are generally moderate, typically ranging between 7 and 12 cm, reflecting the limited number of loading cycles despite the high ground accelerations.

In contrast, far-field earthquakes, including Imperial Valley (1979), Düzce (1999), and Kobe (1995), are characterized by longer shaking durations and a higher number of cyclic loadings. This sustained input of seismic energy provides sufficient time for the gradual accumulation of pore water pressure, which results in comparatively larger volumetric strains and vertical settlements. Field observations confirm this trend, with settlements ranging from 2 cm in Düzce to approximately 40 cm in the reclaimed lands of Kobe, and about 12 cm in Imperial Valley. However, when pile modeling is considered, the magnitude of settlement is expected to be significantly reduced, as illustrated in Figure 11. The maximum settlement corresponds to the Kobe earthquake, with a value of 9 cm, while the minimum settlement is associated with the Imperial Valley earthquake. The explanation

for this variation, as well as the differences between near-field and far-field seismic events, is provided in the following paragraph.

Overall, the comparison indicates that:

- Near-field earthquakes tend to cause smaller but abrupt settlements, often accompanied by localized deformations and ground failures.
- Far-field earthquakes generally result in larger cumulative settlements due to the prolonged shaking duration, despite sometimes having lower peak accelerations.

This distinction is critical for geotechnical earthquake engineering design, as it underlines the necessity of considering not only the intensity but also the duration and frequency content of ground motion when assessing liquefaction-induced settlements.

In general, liquefaction-induced settlement is strongly influenced by the effective stress level, the intensity of ground shaking (PGA or amax ,(and the duration of seismic loading.

Near-Fault Earthquakes:

- Typically characterized by strong but short-duration velocity pulses.
- These earthquakes transfer a large amount of energy within a short time , which can cause a rapid increase in excess pore water pressure and trigger liquefaction suddenly.
- However ,because the shaking duration is relatively short, the final settlement is usually smaller compared to far-field earthquakes, although more severe localized deformations and ground failures may occur.

Far-Field Earthquakes:

- Characterized by longer shaking durations and multiple loading cycles.
- If the shaking intensity (PGA or peak acceleration) increases, the sustained loading allows excess pore water pressure to accumulate progressively.
- As a result, the cumulative liquefaction-induced settlement in far-field earthquakes is generally greater than that observed in near-fault cases.
- In far-field earthquakes, higher shaking intensity leads to larger settlements due to the longer and more numerous cycles of loading.
- In near-fault earthquakes, higher intensity causes a rapid onset of liquefaction and associated settlement, but the total settlement is often smaller than in far-field cases, except very close to the fault where abrupt ground failures and significant displacements may occur.

Summary:

- Near-field earthquakes: smaller overall settlement but more severe localized deformations.
- Far-field earthquakes: larger cumulative settlement due to prolonged shaking duration

10. Conclusion

This study conducted a detailed three-dimensional numerical analysis using FLAC3D to investigate the settlement behavior of pile groups in liquefiable sands under seismic excitation. The results demonstrated that earthquake characteristics, particularly the duration and frequency content of ground motion, play a crucial role in liquefaction development and post-earthquake settlement.

The comparison between near-field and far-field earthquakes revealed distinct behavioral patterns. Near-field events, characterized by strong but short-duration velocity pulses, tend to induce abrupt yet limited settlements. In contrast, far-field motions produce larger cumulative settlements due to prolonged shaking and the gradual accumulation of pore pressure. Vertical ground motion components were found to significantly amplify

settlement, indicating the necessity of their inclusion in seismic design analyses.

From an engineering standpoint, the study underscores the importance of considering both the intensity and duration of seismic loading when assessing pile group performance in liquefiable soils. The findings can aid in improving design codes and optimizing pile spacing and group configurations to mitigate seismic-induced settlement.

Future research should extend the present work by incorporating nonlinear superstructure interaction, different pile materials, and layered soil profiles. Such enhancements would further refine the understanding of soil–pile interaction mechanisms and support the development of more resilient foundation systems in earthquake-prone regions.

11. References

.1 Seed, H.B. and I.M. Idriss, *Simplified procedure for evaluating soil liquefaction potential.* Journal of the Soil Mechanics and Foundations division, 1971. **97**(9): p. 1249-1273.

.2 Holzer, T.L. and T.L. Youd, *Liquefaction, ground oscillation, and soil deformation at the Wildlife Array, California.* Bulletin of the Seismological society of America, 2007. **97**(3): p. 961-976.

.3 Subedi, M. and I.P. Acharya, *Liquefaction hazard assessment and ground failure probability analysis in the Kathmandu Valley of Nepal* .Geoenvironmental Disasters, 2022. **9**(1): p. 1.

.4 Ansari, A., et al., *Liquefaction hazard assessment in a seismically active region of Himalayas using geotechnical and geophysical investigations: a case study of the Jammu Region.* Bulletin of Engineering Geology and the Environment, 2022. **81**(9): p. 349.

.5 Bhattacharya, S., et al., *Collapse of Showa Bridge during 1964 Niigata earthquake: A quantitative reappraisal on the failure mechanisms.* Soil Dynamics and Earthquake Engineering, 2014. **65**: p. 55-71.

.6 Towhata, I., *Review of lessons learnt in 1964 after the Niigata earthquake.* Japanese Geotechnical Society Special Publication, 2024. **10**(10): p. 241-246.

.7 Nuñez Jara, S.A., *Spatial variability of shear wave velocity: Implications dor the liquefaction response of a case study from the 2010 Maule Mw 8.8 earthquake, Chile.* 2024.

.8 Mijic, Z. and J.D. Bray, *Insights from liquefaction ejecta case histories for the 2010–2011 Canterbury earthquakes.* Soil Dynamics and Earthquake Engineering, 2024. **176**: p. 108267.

.9 Khosravi, M. and S. Zaregarizi, *Liquefaction potential and sediment ejecta manifestation of thinly interbedded sands and fine-grained soils: Palinurus road site in Christchurch subjected to 2010–2011 Canterbury earthquake sequence.* Journal of Geotechnical and Geoenvironmental Engineering, 2024. **150**(5): p. 04024026.

.10 Towhata, I., *Summary of geotechnical activities in response to the 2011 Tohoku earthquake; follow-up of my TC203 Ishihara Lecture in 2019.* Soil Dynamics and Earthquake Engineering, 202 :164 .3p. 107640.

.11 Arango-Serna, S., et al., *New seismic monitoring center in South America to assess the liquefaction risk posed by subduction earthquakes.* Journal of Seismology, 2023. **27**(3): p. 385-407.

.12 Minarelli, L., et al., *Liquefied sites of the 2012 Emilia earthquake: a comprehensive database of the geological and geotechnical features (Quaternary alluvial Po plain, Italy).* Bulletin of Earthquake Engineering, 2022. **20**(8): p. 3659-3697.

.13 Pratama, A., T. Fathani, and I. Satyarno. *Liquefaction potential analysis on Gumbasa Irrigation Area in Central Sulawesi Province after 2018 earthquake*. in *IOP Conference Series: Earth and Environmental Science*. 2021. IOP Publishing.

.14 Ohsaki, Y., *Niigata earthquakes, 1964 building damage and soil condition.* Soils and Foundations, 1966. **6**(2): p. 14-37.

.15 Omarov, M., *Liquefaction potential and post-liquefaction settlement of saturated clean sands: And effect of geofiber reinforcement*. 2010.

.16 Martin, G.R., H.B. Seed, and W.L. Finn, *Fundamentals of liquefaction under cyclic loading.* Journal of the geotechnical engineering division, 1975. **101**(5): p. 423-438.

.17 Seed, H.B., I.M. Idriss, and I. Arango, *Evaluation of liquefaction potential using field performance data.* Journal of geotechnical engineering :(3)109 .1983 ,p. 458-482.

.18 Montoya, B.M., J.T. DeJong, and R.W. Boulanger. *Dynamic response of liquefiable sand improved by microbial-induced calcite precipitation*. in *Bio-and chemo-mechanical processes in geotechnical engineering: Géotechnique symposium in print 2013*. 2014. ICE Publishing.

.19 Kumari, D. and W.-N. Xiang, *Review on biologically based grout material to prevent soil liquefaction for ground improvement.* International Journal of Geotechnical Engineering, 2019. **13**(1): p. 48-53.

.20 Gowda ,G., et al., *Effect of Liquefaction Induced Lateral Spreading on Seismic Performance of Pile Foundations.* Civil Engineering Journal, 2022. **7**: p. 58-70.

.21 Dhakal, R., M. Cubrinovski, and J.D. Bray, *Geotechnical characterization and liquefaction evaluation of gravelly reclamations and hydraulic fills (Port of Wellington, New Zealand).* Soils and Foundations, 2020. **60**(6): p. 1507-1531.

.22 Esfeh, P.K. and A.M. Kaynia, *Numerical modeling of liquefaction and its impact on anchor piles for floating offshore structures.* Soil Dynamics and Earthquake Engineering, 2019. **127**: p. 105839.

.23 Ahmadi, M.M., et al., *Effects of loading frequency on soil–pile interaction using numerical nonlinear three-dimensional analyses.* International Journal of Geomechanics, 2025. **25** :(1)p. 04024301.

.24 Zhong, C., Z. Chen, and J. Zhou, *Numerical Investigations of Pile Group Foundations under Different Pile Length Conditions.* Applied Sciences, 2024. **14**(5): p. 1908.

.25 Maheshwari, B. and M. Firoj, *Seismic response of combined piled raft foundation using advanced liquefaction model.* Soil Dynamics and Earthquake Engineering, 2024. **181**: p. 108694.

.26 Souri, M., et al., *Numerical modeling of a pile-supported wharf subjected to liquefaction-induced lateral ground deformations.* Computers and Geotechnics, 2023. **154**: p. 105117.

.27 Russo, G., G. Marone, and L. Di Girolamo, *Hybrid energy piles as a smart and sustainable foundation.* Journal of Human, Earth, and Future, 2021. **2**(3): p. 306-322.

.28 Basavanagowda, G., et al. *Behavior of pile group in liquefied soil deposits under earthquake loadings*. in *Seismic Design and Performance: Select Proceedings of 7th ICRAGEE 2020*. 2021. Springer.

.29 Kwon, S.Y. and M. Yoo, *Study on the dynamic soil-pile-structure interactive behavior in liquefiable sand by 3D numerical simulation.* Applied Sciences, 2020. **10**(8): p. 2723.

.30 Rollins, K. and J. Hollenbaugh. *Liquefaction induced negative skin friction from blast-induced liquefaction tests with auger-cast piles*. in *Procs., 6th Intl. Conf. on Earthquake Geotechnical Engineering, Christchurch, New Zealand, New Zealand Geotechnical Society*. 2015.

.31 Chatterjee, K. and D. Choudhury. *DYNAMIC ANALYSIS OF PILE GROUP IN LIQUEFIABLE SOIL USING FLAC3D*. in *Proceedings of the 5th Indian Young Geotechnical Engineers Conference (5IYGEC): Extended Abstracts*. 2015. Shweta Publications.

.32 Su, D. and X.-s. Li, *Centrifuge investigation on seismic response of single pile in liquefiable soil.* CHINESE JOURNAL OF GEOTECHNICAL ENGINEERING-CHINESE EDITION-, 2006. **28**(4): p. 423.

.33 Rollins, K. and S. Strand. *Downdrag forces due to liquefaction surrounding a pile*. in *Proc., 8th National Conf. on Earthquake Engineering*. 2006. Earthquake Engineering Research Institute.

.34 Elgamal, A., J. Lu, and Z. Yang, *Liquefaction-induced settlement of shallow foundations and remediation: 3D numerical simulation.* Journal of earthquake engineering, 2005. **9**(spec01): p. 17-45.

.35 De Alba, P.A., *Pile settlement in liquefying sand deposit.* Journal of Geotechnical Engineering, 1983. **109**(9): p. 1165.1180-

.36 Chi, M., et al., *Numerical and experimental modeling dynamic responses of permeable pile in liquefiable sand ground*.

.37 Reyes, A., M. Taiebat, and S. Zarnani, *Application of SANISAND-MSf Constitutive Model for Simulating Cyclic Liquefaction in FLAC2D and FLAC3D*.

.38 Youd, T.L. and I.M. Idriss, *Liquefaction resistance of soils: summary report from the 1996 NCEER and 1998 NCEER/NSF workshops on evaluation of liquefaction resistance of soils.* Journal of geotechnical and geoenvironmental engineering, 2001. **127**(4): p. 297-313.

.39 Bhattacharya, S. and M. Bolton. *Buckling of piles during earthquake liquefaction*. in *Proc. 13th world conference on earthquake engineering*. 2004.

.40 Tokimatsu, K. and Y. Asaka, *Effects of liquefaction-induced ground displacements on pile performance in the 1995 Hyogoken-Nambu earthquake.* Soils and Foundations, 1998. **38**: p. 163-177.

.41 Ishihara, K. and M. Yoshimine, *Evaluation of settlements in sand deposits following liquefaction during earthquakes.* Soils and foundations :(1)32 .1992 ,p. 173-188.

.42 Tokimatsu, K. and H.B. Seed, *Evaluation of settlements in sands due to earthquake shaking.* Journal of geotechnical engineering, 1987. **113**(8): p. 861-878.

.43 Boulanger, R.W. and I. Idriss, *Probabilistic standard penetration test–based liquefaction–triggering procedure.* Journal of Geotechnical and Geoenvironmental Engineering, 2012. **138**(10): p. 1185-1195.

.44 Cetin, K.O., et al., *Standard penetration test-based probabilistic and deterministic assessment of seismic soil liquefaction potential.* Journal of geotechnical and geoenvironmental engineering, 2004. **130**(12): p. 1314-1340.

.45 Code, B.B., *Building officials and code administrators.* International (BOCA), 1973.

.46 Focht Jr, J. and M. ONeill. *Piles and other deep foundations*. in *International conference on soil mechanics and foundation engineering*. *11*. 1985.

.47 Haldar, S. and G.S. Babu, *Failure mechanisms of pile foundations in liquefiable soil: Parametric study.* International Journal of Geomechanics, 2010. **10**(2): p. 74-8.4

.48 Liyanapathirana, D.S. and H. Poulos, *Pseudostatic approach for seismic analysis of piles in liquefying soil.* Journal of Geotechnical and Geoenvironmental Engineering, 2005. **131**(12): p. 1480-1487.